

Prediction of LSE via Reaction Dispersion

D. Devi Sirisha, Satya Naresh

Abstract—A dispersion term is hosted into LSE, resulting in a RD-LSE equation, to which a piecewise constant solution can be derived. This project presents an innovative reaction-dispersion (RD) method for implicit active outlines, which is completely free of the costly re-initialization procedure in level set evolution (LSE). In order to have a balanced statistical result of the RD based LSE, we recommend a two-step splitting method (TSSM) to iteratively crack the RD-LSE equation: first iterating the LSE equation, and then solving the dispersion equation. The second step regularizes the level set function obtained in the first step to ensure stability, and thus the complex and costly re-initialization procedure is completely eliminated from LSE. By successfully applying dispersion to LSE, the RD-LSE model is stable by means of the simple finite difference method, which is very easy to implement. The proposed RD method can be generalized to solve the LSE for both variation level set method and PDE-based level set method. The RD-LSE method shows appropriate noble concert on boundary anti-leakage, and it can be voluntarily prolonged to high dimensional level set method. The extensive and promising experimental results on synthetic and real images validate the effectiveness of the proposed RD-LSE approach.

Keywords: RD-LSE, PDE, TSSM.

I. INTRODUCTION

In recent years, a large body of work on geometric active contours, i.e., active contours implemented via level set methods, has been proposed to address a wide range of image segmentation problems in image processing and computer vision (cf. [3, 5, 7]). Level set methods were first introduced by Osher and Sethian [11] for capturing moving fronts. Active contours were introduced by Kass, Witkins, and Terzopoulos [1] for segmenting objects in images using dynamic curves. The existing active contour models can be broadly classified as either parametric active contour models or geometric active contour models according to their representation and implementation. In particular, the parametric active contours [1, 2] are represented explicitly as parameterized curves in a Lagrangian framework, while the geometric active contours [5–7] are represented implicitly as level sets of a two-dimensional function that evolves in an Eulerian framework. Vision is the most advanced sense among the five senses of human beings, and plays the most important role in human perception. Although the sensitivity of human vision is limited within the visible band, imaging machines can operate on the images generated by sources that human vision cannot associate with. Thus, machine vision encompasses a wide and varied field of applications, even in areas where human vision cannot function, e.g. infrared (IR), ultraviolet (UV), X-ray, magnetic resonance imaging (MRI), ultrasound.

Although there is no clear distinction among image processing, image analysis, and computer vision, usually they are considered as hierarchies in the processing continuum. The low-level processing, which involves primitive operations such as noise filtering, contrast enhancement, and image sharpening, is considered as image processing. Note both its inputs and outputs are images. The mid-level processing, which involves segmentation and pattern classification, is considered as image analysis or image understanding [1]. Note its input generally are images, but its outputs are attributes extracted from those images, e.g. edges, contours, and the identity of individual objects, called class. The high-level processing, which involves ‘making sense’ of an ensemble of recognized objects and performing the cognitive functions at the far end of the processing continuum, is considered as computer vision [1]. We discuss the technologies used in the image analysis, and propose novel segmentation methods through this document. Geometric active contours are independently introduced by Caselles et al.[5] and Malladi et al.[7], respectively. These models are based on curve evolution theory [10] and level set method [17]. The basic idea is to represent contours as the zero level set of an implicit function defined in a higher dimension, usually referred as the level set function, and to evolve the level set function according to a partial differential equation (PDE). This approach presents several advantages [4] over the traditional parametric active contours. First, the contours represented by the level set function may break or merge naturally during the evolution, and the topological changes are thus automatically handled. Second, the level set function always remains a function on a fixed grid, which allows efficient numerical schemes. Early geometric active contour models (cf. [5–7]) are typically derived using a Lagrangian formulation that yields a certain evolution PDE of a parametrized curve. This PDE is then converted to an evolution PDE for a level set function using the related Eulerian formulation from level set methods. As an alternative, the evolution PDE of the level set function can be directly derived from the problem of minimizing a certain energy functional defined on the level set function. This type of variational methods are known as variational level set methods [8, 9, 14]. Compared with pure PDE driven level set methods, the variational level set methods are more convenient and natural for incorporating additional information, such as region-based information [8] and shape-prior information [9], into energy functionals that are directly formulated in the level set domain, and therefore produce more robust results. For examples, Chan and Vese [8] proposed an active contour model using a variational level set formulation. By incorporating region-based information into their energy functional as an additional constraint, their model has much larger convergence range and flexible initialization. Vemuri and Chen [9] proposed another variational level set formulation.

Manuscript published on 30 October 2014.

* Correspondence Author (s)

D. Devi Sirisha, M. Tech Student. D/O D Trimurthulu, D. No 5-522, Near KIMS Hospital, Andhra Pradesh, Amalapuram, India.

CH. Satya Naresh, Assistant Professor, D/O D Trimurthulu, D. No 5-522, Near KIMS Hospital, Andhra Pradesh, Amalapuram, India.

© The Authors. Published by Blue Eyes Intelligence Engineering and Sciences Publication (BEIESP). This is an open access article under the CC-BY-NC-ND license <http://creativecommons.org/licenses/by-nc-nd/4.0/>

By incorporating shape-prior information, their model is able to perform joint image registration and segmentation.

II. EDGE DETECTION FOR IMAGES

Edges are boundaries between different textures. Edge also can be defined as discontinuities in image intensity from one pixel to another. The edges for an image are always the important characteristics that offer an indication for a higher frequency. Detection of edges for an image may help for image segmentation, data compression, and also help for well matching, such as image reconstruction and so on. There are many methods to make edge detection. The most common method for edge detection is to calculate the differentiation of an image. The first-order derivatives in an image are computed using the gradient, and the second-order derivatives are obtained using the Laplacian. Another method for edge detection uses Hilbert Transform. And we have proposed a new method called short response Hilbert transform (SRHLT) that combines the differentiation method and the Hilbert transform method. However, SRHLT improved the differentiation method and HLT, it still cannot fulfil our request. We can view SRHLT as the medium between the differentiation operation and the Hilbert transform (HLT) for edge detection. Now, we will introduce improved harris' algorithm and new corner detection algorithm. A more accurate algorithm for corner and edge detections that is the improved form of the well-known Harris' algorithm is introduced. First, instead of approximating $|L[m+x, n+y]-L[m, n]|^2$ just in terms of x^2 , xy , and y^2 , we will approximate $|L[m+x, n+y]-L[m, n]|(L[m+x, n+y]-L[m, n])$ by the linear combination of x^2 , xy , y^2 , x , y , and 1 . There are 6 basis different from 3 basis. We can observe the sign of variation with this modification. It can avoid misjudging the pixel at the wrong location and is also helpful for increasing the robustness to noise. Moreover, we also use orthogonal polynomial expansion and table looking up and define the corner as the "integration" of the quadratic function to further improve the performance. From simulations, our algorithm is effective both for corner detection and edge detection.

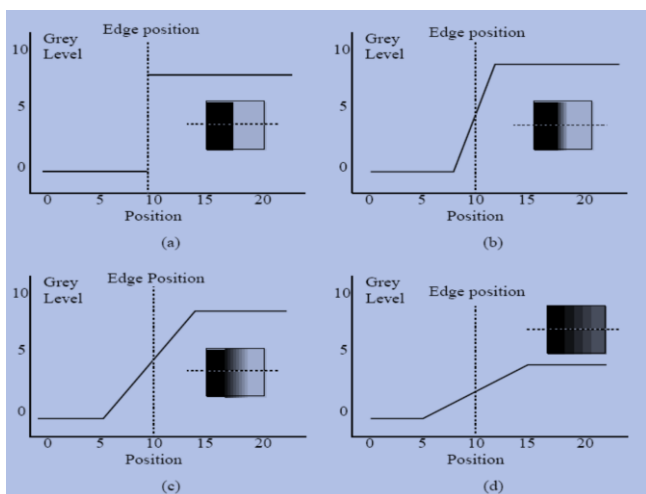


Fig. 1: Step edges. (a) The change in level occurs exactly at pixel 10. (b) The same level change as before, but over 4 pixels centred at pixel 10. This is a ramp edge. (c) Same level change but over 10 pixels, centred at 10. (d) A smaller change over 10 pixels. The insert shows the way

the image would appear, and the dotted line shows where the image was sliced to give the illustrated cross-section

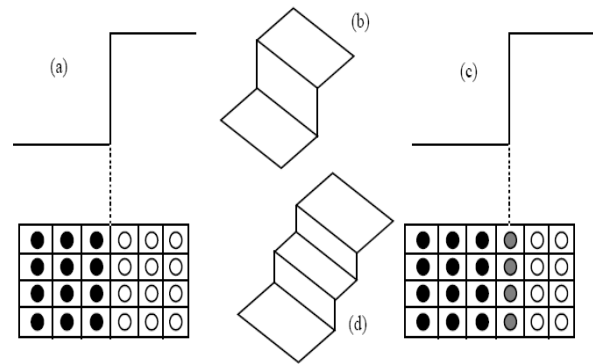


Fig. 2: The effect of sampling on a step edge. (a) An ideal step edge. (b) Three dimensional view of the step edge. (c) Step edge sampled at the centre of a pixel, instead of on a margin. (d) The result, in three dimensions, has the appearance of a staircase

III. FIRST-ORDER DERIVATIVE EDGE DETECTION

$$\nabla \mathbf{f} = \begin{bmatrix} G_x \\ G_y \end{bmatrix} = \begin{bmatrix} \frac{\partial f}{\partial x} \\ \frac{\partial f}{\partial y} \end{bmatrix}. \quad (4.1)$$

An important quantity in edge detection is the magnitude of this vector, denoted $|\nabla \mathbf{f}|$, Where

$$|\nabla \mathbf{f}| = \sqrt{G_x^2 + G_y^2}. \quad (4.2)$$

Another important quantity is the direction of the gradient vector. That is,

$$\text{angle of } \nabla \mathbf{f} = \tan^{-1} \left(\frac{G_y}{G_x} \right) \quad (4.3)$$

IV. ALGORITHM

a) First-Order Derivative Edge Detection:

An important quantity in edge detection is the magnitude of this vector, denoted $|\nabla \mathbf{f}|$, where

$$\nabla \mathbf{f} = \begin{bmatrix} G_x \\ G_y \end{bmatrix} = \begin{bmatrix} \frac{\partial f}{\partial x} \\ \frac{\partial f}{\partial y} \end{bmatrix} \quad (4.27)$$

The magnitude gives the maximum rate of increase of $f(x, y)$ per unit distance in the direction of $\nabla \mathbf{f}$.

$$|\nabla \mathbf{f}| = \sqrt{G_x^2 + G_y^2} \quad (4.28)$$

Another important quantity is the direction of the gradient vector. That is,

$$\text{angle of } \nabla f = \tan^{-1} \left(\frac{G_y}{G_x} \right) \quad (4.29)$$

Where the angle is measured with respect to the x-axis. The direction of an edge at (x, y) is perpendicular to the direction of the gradient vector at that point. Computation of the gradient of an image is based on obtaining the partial derivatives of $\partial f / \partial x$ and $\partial f / \partial y$ at every pixel location.

b) Sobel Edge Detection:

P1	P2	P3
P4	P5	P6
P7	P8	P9

Fig. 3: A 3x3 Area of an Image

-1	-2	-1
0	0	0
1	2	1

-1	0	1
-2	0	2
-1	0	1

Fig. 4: The Sobel Operators

$$|G| = |G_x| + |G_y|$$

$$|(P_1 + 2P_2 + P_3) - (P_7 + 2P_8 + P_9)| + |(P_3 + 2P_5 + P_9) - (P_1 + 2P_4 + P_7)|$$

We can use G_x and G_y convolve the image then we can get the gradient by equation and equation.

c) Canny Edge Detection:

It is hard to find the gradient by using equation

$$G(x) = e^{-\left(\frac{x^2}{2\sigma^2}\right)} \quad (4.31)$$

In order to simplify the computation, we adapt another equation equal to the equation, this equation is first-order derivative function of Gaussian function.

$$G'(x) = \left(-\frac{x}{\sigma^2}\right) e^{-\left(\frac{x^2}{2\sigma^2}\right)} \quad (4.32)$$

Because the computation of 2-dimension convolution is complex and large. We find the gradient by convolve x-direction and y-direction individually in fact as below:

$$M_x(x, y) = \dot{G}_x * I(x, y)$$

$$M_y(x, y) = \dot{G}_y * I(x, y) \quad (4.34)$$

d) Second-Order Derivative Detection:

The Laplacian of a 2-D function f (x, y) is a second-order derivative defined as

$$\nabla^2 f = \frac{\partial^2 f}{\partial x^2} + \frac{\partial^2 f}{\partial y^2} \quad (4.35)$$

There are two digital approximations to the Laplacian for a 3x3 region:

$$\nabla^2 f = 4z_5 - (z_2 + z_4 + z_6 + z_8) \quad (4.36)$$

$$\nabla^2 f = 8z_5 - (z_1 + z_2 + z_3 + z_4 + z_6 + z_7 + z_8 + z_9) \quad (4.37)$$

Where the z's are Masks for implementing equations

0	-1	0
-1	4	-1
0	-1	0

(a)

-1	-1	-1
-1	8	-1
-1	-1	-1

Fig. 5: Two kind of 3x3 Laplacian Mask

The Laplacian is usually combined with smoothing as a precursor to finding edges via zero-crossings. The 2-D Gaussian function

$$h(x, y) = -e^{-\frac{x^2+y^2}{2\sigma^2}} \quad (4.38)$$

Where σ is the standard deviation, blurs the image with the degree of blurring being determined by the value of σ . The Laplacian of h is

$$\nabla^2 h(x, y) = -\left[\frac{x^2 + y^2 - 2\sigma^2}{\sigma^4} \right] e^{-\frac{r^2}{2\sigma^2}} \quad (4.39)$$

This function is commonly referred to as the Laplacian of Gaussian (LOG).

0	0	0	-1	-1	-2	-1	-1	0	0	0
0	0	-2	-4	-8	-9	-8	-4	-2	0	0
0	-2	-7	-15	-22	-23	-22	-15	-7	-2	0
-1	-4	-15	-24	-14	-1	-14	-24	-15	-4	-1
-1	-8	-22	-14	52	103	52	-14	-22	-8	-1
-2	-9	-23	-1	103	178	103	-1	-23	-9	-2
-1	-8	-22	-14	52	103	52	-14	-22	-8	-1
-1	-4	-15	-24	-14	-1	-14	-24	-15	-4	-1
0	-2	-7	-15	-22	-23	-22	-15	-7	-2	0
0	0	-2	-4	-8	-9	-8	-4	-2	0	0
0	0	0	-1	-1	-2	-1	-1	0	0	0

Fig. 6: An 11x11 mask approximation to Laplacian of Gaussian (LOG)



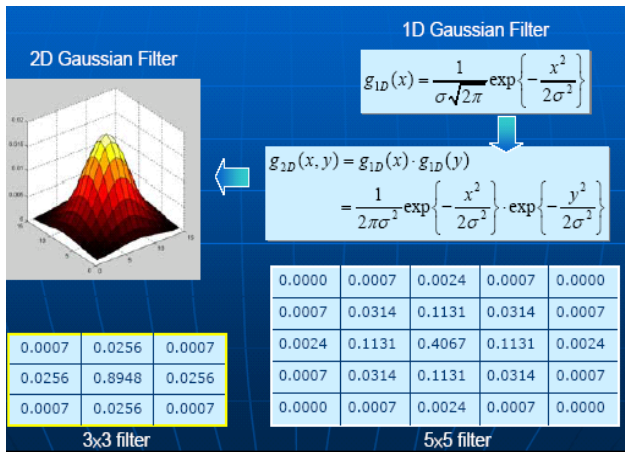


Fig. 7: 1D & 2D Gaussian Filters

Because second-order derivative operator is sensitive to noise, we use low-pass filter to eliminate the noise first. We combine Gaussian filter with Laplacian operator so that we get Laplacian of Gaussian Edge Detector. We take advantage of the property of Gaussian function to distribute the noise.

e) **Hilbert Transform for Edge Detection:**

There is another method for edge detection that uses the Hilbert transform (HLT). The HLT is

$$g_H(\tau) = h(x) * g(x), \quad \text{where } h(x) = \frac{1}{\pi x} \quad (4.40)$$

Here * means convolution. Alternatively,

$$G_H(f) = H(f)G(f) \quad (4.41)$$

Where $G(f) = FT[g(x)]$ (FT means the Fourier transform), $G_H(f) = FT[g_H(x)]$, and

$$H(f) = -j \operatorname{sgn}(f), \quad (4.42)$$

where the sign function is defined as

$$\begin{aligned} \operatorname{sgn}(f) &= 1 \text{ when } f > 0, \\ \operatorname{sgn}(f) &= -1 \text{ when } f < 0, \\ \operatorname{sgn}(0) &= 0 \end{aligned} \quad (4.43)$$

f) **Short Response Hilbert Transform for Edge Detection:**

Based on Canny's criterion [5], we develop the short response Hilbert transform (SRHLT), which is the intermediate of the original HLT and the differentiation operation. For edge detection, the SRHLT can compromise the advantages of the HLT and differentiation. It can well distinguish the edges from the non-edge regions and at the same time are robust to noise. We also find that there are many ways to define the SRHLT. If the constraints which come from Canny's criterion are satisfied, the resultant SRHLT will have good performance in edge detection.

V. **SEGMENTATION METHOD**

Segmentation process consists of several steps. The first of all is input image conversion to chosen feature space, which may depends of used clustering method. In our case is input image converted from RGB color space to $L^*u^*v^*$ color space and L^* , u^* and v^* values are features respectively

attributes for fuzzy c-means clustering method. Next step after input image conversion to feature space is applied clustering. In our case, we have chosen fuzzy c-means clustering method, settings are in experiments section. After these two steps (input image conversion to feature space of clustering method and accomplishing clustering method) is accomplished next segmentation method.

VI. **METHOD 1 (M1)**

BEGIN OF M1

Assumptions: Image transformed into feature space, number of clusters c , stop condition ϵ , fuzziness parameter m .

Step 1: Cluster image in feature space, with next conditions: number of clusters is c , fuzziness index is m and stop condition is ϵ .

Step 2: Repeat for each pixel ija of image I .

Step 2.1: Find out, into which cluster C belongs pixel ija most.

Step 2.2: Find out, whether in the closest surroundings of pixel ija exists segment kR , which points belong to same cluster C .

Step 2.3: If such segment kR exists, than pixel ija add to segment kR , else create new segment nR and add pixel ija to new segment nR .

Step 3: Merge all segments, which belong to one cluster and are neighbours.

Step 4: Arrange borders of all segments.

END OF M1

Segmentation method used in experiments is based on simple region growing method. Method was used in [2, 4, 6] and in this paper is marked as method M1. In [2] was used with simple defuzzification rule, in [4] was this method enhanced with thresholding parameter T and in [6] was used with another defuzzification rule. Method M2: is segmentation method based on method M1, but method M2 uses extended feature space, which will be described in next section. Difference between method M1 and M2 will be only feature space.

VII. **EXTENSION OF FEATURE SPACE OF FUZZY C-MEANS**

The most important part of this segmentation method is extension of feature space. Extension of feature space is based on simple idea, that neighbouring pixels have approximately same values of lightness and chroma. But in real images, noise is corrupting the image data or image usually consists of textured segments. Basic segmentation methods based on fuzzy c-means clustering are working as follows:

1. Convert image into feature space of clustering method (usually is used RGB color space, but IHS, HLS, $L^*u^*v^*$ or $L^*a^*b^*$ color spaces are used too).
2. Run fuzzy c-means method on converted image.
3. Use some defuzzification rule or rules to classify each pixel to segment.

Simple defuzzification rule is based on maximal membership grade of pixel to cluster [1, 4]. Basic feature space is only color space, e.g.



RGB, HIS, HLS or $L^*u^*v^*$ color spaces as shown on Fig. 4.17. This feature spaces in combination with clustering methods have one big disadvantage. In clustering process is not involved information about pixels in neighbourhood, which results in bad segmentation results, because of noise or texture.

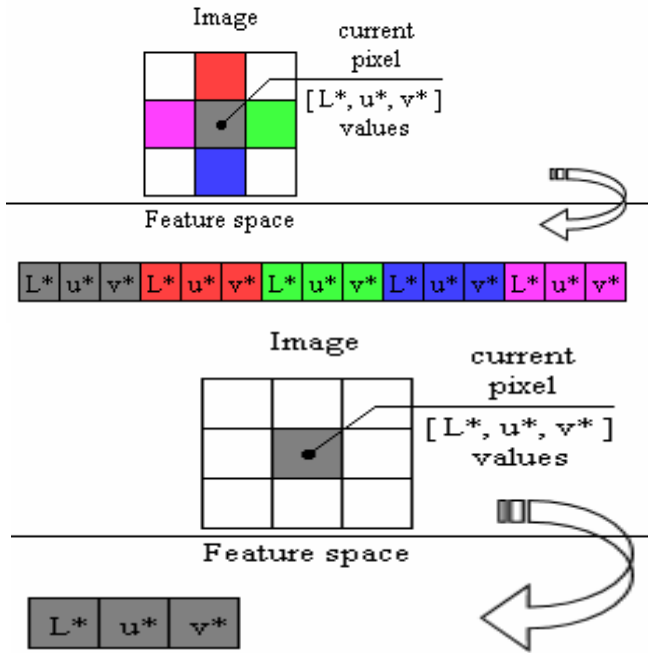
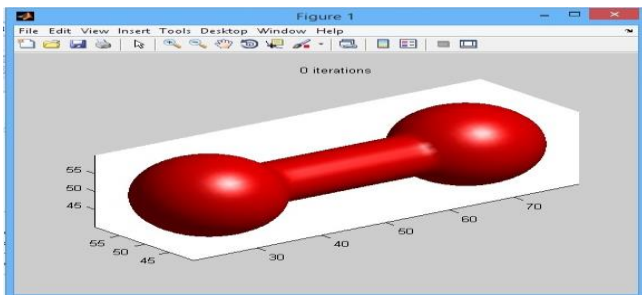


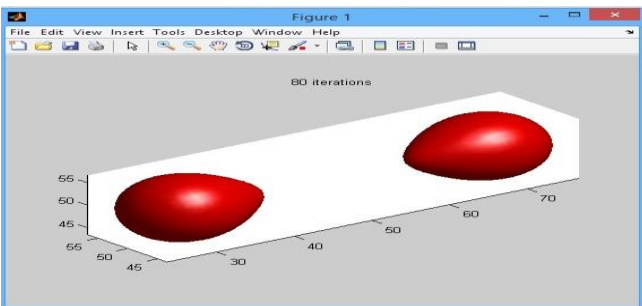
Fig. 8: Extension of Feature Space

Extension of feature space is based on involving of neighbouring pixels 'information. One pixel has 15 instead of 3 features. In simple case [2, 4, 6] has pixel only 3 features ($L^*u^*v^*$ values, Figure). In our modification has pixel 15 features, its own $L^*u^*v^*$ values and $L^*u^*v^*$ values of its neighbours. In practical implementation of this extension was used next sequence of pixels: current pixel, up, right, down and left neighbour pixel.

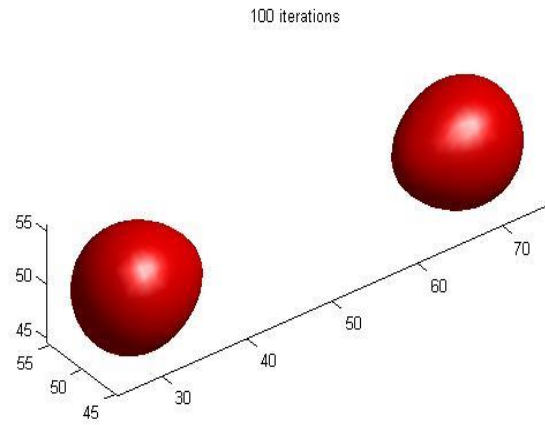
VIII. OUTPUTS



(a)

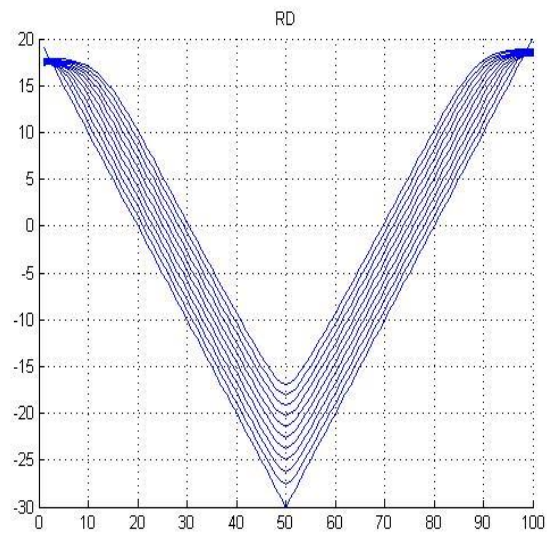


(b)

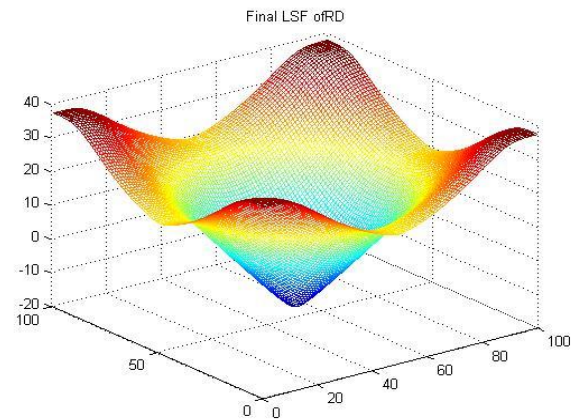


(c)

Fig. 9: Motion of dumbbell driven by mean curvature at different iterations



(a)



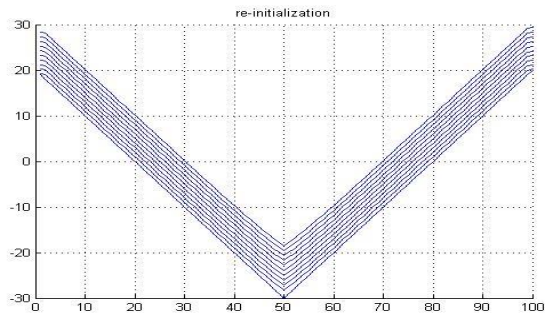
(b)

IX. CONCLUSION

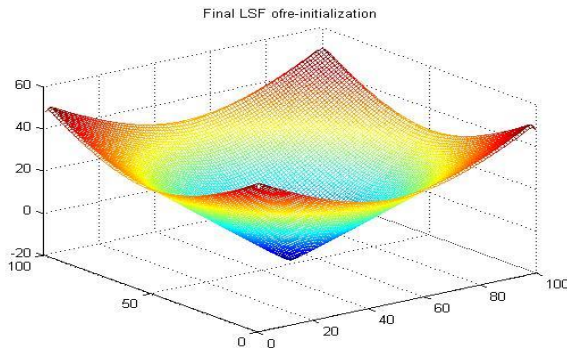
In traditional image analysis, image segmentation performs a role of pre-processing for pattern classification providing the input data. We have integrated image segmentation and statistical pattern classification by using the statistical distribution of image intensity as the feature used in image segmentation. Thus, the proposed image segmentation methods produce the result of statistical pattern classification as well as image segmentation reducing the computation time and effort. Although these initializations are very different, the final contours are almost the same, which validates that our RD method can robustly evolve to the global minimum of the energy functional, leading a good global segmentation. The performance of the re-initialization and GDRLSE methods fluctuates significantly for the noise with different strength. However, the JS value by our RD method does not change much, which demonstrates the robust anti-noise performance of RD. we proposed a reaction-diffusion (RD) based level set evolution (LSE), which is completely free of the re-initialization procedure required by traditional level set methods. A two-step-splitting-method (TSSM) was then proposed to effectively solve the RD based LSE. The proposed RD method can be generally applied to either variational level set methods or PDE-based level set methods. It can be implemented by using the simple finite difference scheme.

REFERENCES

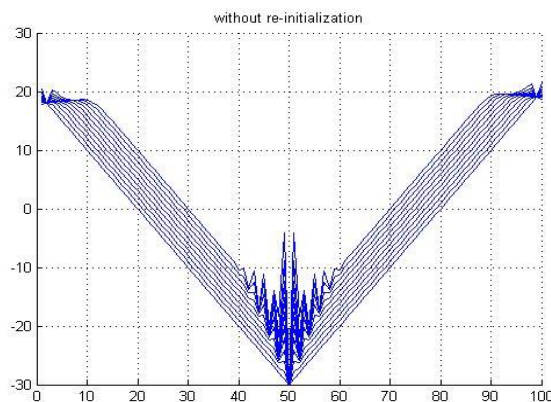
- [1] S. Zhu and A. Yuille, "Region competition: unifying snakes, region growing, and Bayes/MDL for multiband image segmentation," IEEE Trans. Pattern Analysis and Machine Intelligence, vol. 18, no. 9, pp. 884-900, 1996.
- [2] K. Zhang, L. Zhang, H. Song and W. Zhou, "Active contours with selective local or global segmentation: a new formulation and level set method," Image and Vision Computing, vol. 28, issue 4, pp. 668-676, April 2010.
- [3] M. Sussman, P. Smereka, S. Osher, "A Level Set Approach for Computing Solutions to Incompressible Two-Phase Flow," J. Comp. Phys., vol. 114, pp. 146-159, 1994.
- [4] D. Adalsteinsson and J. Sethian, "A fast level set method for propagating interfaces," J. Comput. Phys., vol. 118, no. 2, pp. 269-277, 1995.
- [5] R. Tsai, and S. Osher, "Level Set Methods and Their Applications in Image Science," COMM.MATH.SCI., vol.1, no. 4, pp. 623-656, 2003.
- [6] S. Esedoglu, and Y. Tsai, "Threshold dynamics for the piecewise constant Mumford-Shah functional," J. Comp. Phys., vol. 211, pp. 367-384, 2006.
- [7] T. Chan and L. Vese, "Active contours without edges," IEEE Trans. Image Process, vol. 10, no. 2, pp. 266-277, Feb. 2001.
- [8] G. Aubert and P. Kornprobst, Mathematical problems in image processing, New York: Springer-Verlag, 2000
- [9] J. Rubinstein, P. Sternberg, and J. Keller, "Fast reaction, slow diffusion, and curve shortening," SIAM J.APPL.MATH, Vol. 49, No. 1, pp. 116-133, Feb. 1989.
- [10] P. Sternberg, "The effect of a singular perturbation on nonconvex variational problems," Arch.Rational Mech.Anal., vol. 101, pp. 209-240, 1988.
- [11] L. Evans, Partial Differential Equations, Providence: American Mathematical Society, 1998.
- [12] J. Xu, H. Zhao, "An Eulerian Formulation for Solving Partial Differential Equations Along a Moving Interface," J. Sci. Comp., vol. 19, pp. 573-594, 2003.
- [13] J. Strikwerda, Finite difference schemes and partial differential equations, Wadsworth & Brooks/Cole Advanced Books & Software, Pacific grove, California, 1989.



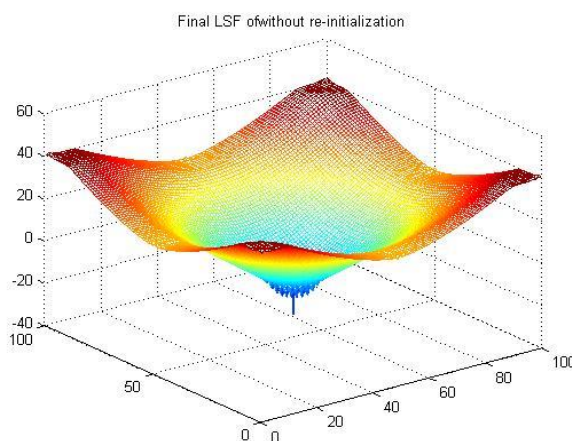
(c)



(d)



(e)



(f)

Fig. 10: Top row: the final LSFs. Bottom row: the middle slices of the LSFs in iterations. From left to right: results by RD method, re-initialization method and the direct implementation without re-initialization

- [14] S. Allen and J. Cahn, "A Microscopic Theory for Antiphase Boundary Motion and Its Application to Antiphase Domain Coarsening," *Acta Metallurgica.*, vol. 27, pp. 1085-1095, 1979.
- [15] S. Baldo, "Minimal Interface Criterion for Phase Transitions in Mixtures of Cahn-Hilliard Fluids," *Annals Inst. Henri Poincare.*, vol. 7, pp. 67-90, 1990.